Dalton Transactions

Accepted Manuscript

ROYAL SOCIETY OF CHEMISTRY

www.rsc.org/dalton

A series of MOFs based on a triangle ligand tri(4-pyridylphenyl)amine combined with carboxylate or nitrate auxiliary ligand

Fandian Meng, Mingdao Zhang, Kang Shen, Yizhi Li and Hegen Zheng*

Dedicated to Professor Xin-Quan Xin on the occasion of his 80th birthday

State Key Laboratory of Coordination Chemistry, School of Chemistry and Chemical Engineering, Nanjing National Laboratory of Microstructures, Nanjing University, Nanjing 210093, P. R. China

A series of new metal-organic frameworks (MOFs) that have novel structures and features based on a triangle ligand tri(4-pyridylphenyl)amine (TPPA), namely $[Co_2(TPPA)_2(1,3\text{-bdc})_2(H_2O)]_n$ (**1**); $[Zn(TPPA)(1,3\text{-bdc})]_n$ (**2**); $[Zn_6(TPPA)_2(betc)(Hbetc)_2(H_2betc)(H_2O)_6{\cdot}7H_2O{\cdot}2DMA]_n$ (**3**); $[Cu(TPPA)(NO_3)_2(H_2O)]{\cdot}2H_2O]_n$ (**4**) (1,3-H_2bdc = 1,3-benzenedicarboxylic acid, betc = 1,2,4,5-benzenetetracarboxylic dianhydride) have been synthesized under solvothermal conditions. In our work, different MOFs are synthesized with different metal ions and in different solvents, guiding to varieties of coordination modes and structures. In addition, photochemical properties of compounds **1**-**4** and the ligands in the solid state have been studied.

Introduction

In recent years, MOFs have been increasingly interested by many inorganic chemists for their charming structures and potential applications, for instance, gas absorption[1], gas separation[2], hydrogen storage[3], molecular magnets[4], catalysis[5], solvatochromic behavior[6], etc. The characters of MOFs are influenced by many factors, such as metal ions[7], ancillary ligands[8], solvents, reaction temperature[9], etc[10-11].

MOFs can be built up by metal ions and carboxylic acid or nitrogen-containing ligands. Compared with polycarboxylic acid, nitrogen-containing ligands have some advantages[12]. In most situations, the N-containing ligands are electrically neutral, while the carboxylate ligands are negatively charged. Moreover, the coordination sites of the N-containing ligands are located in the aromatic rings, which cannot rotate freely, quite different from that of carboxylic acid ligands.[13] Nitrogen-containing ligands can appeal many different coordinate modes, for instance, monodentate, bidentate or chelating[14]. Up to now, pyridine-containing ligands accounted for the largest proportion of nitrogen-containing ligands in the MOF system[15]. Triphenylamine is a triangle substance. In order to build up triangle ligands, nitrogen-containing rings are introduced to triphenylamine[16]. Tris(4-(1H-imidazol-1-yl)phenyl)amine (TIPA) have many interesting characters, for example, a 54-fold interpenetration MOF is built up by Cu^{2+} and TIPA. [17]

Herein, we connect a pyridine ring to triphenylamine, building up a ligand tri(4-pyridylphenyl)amine (TPPA). For the N atom locates on the axes of benzene-pyridine arms, the TPPA ligand is "semi-rigid". Combined with polycarboxylic acid or even inorganic salts, a variety of MOFs are built up. Some MOFs based on TPPA have been already synthesized in our previous work, for example, $\{[Zn(TPPA)(suc)]\cdot 5(H_2O)\cdot DMA\}_n$, a solvent accessible MOF with void space as large as 37.6%.[18] In this paper, four new compounds were obtained under solvothermal conditions, namely $[Co_2(TPPA)_2(1,3\text{-bdc})_2(H_2O)]_n$ (**1**), $[Zn(TPPA)(1,3\text{-bdc})]_n$ (**2**), $[Zn_6(TPPA)_2(betc)(Hbetc)_2(H_2betc)(H_2O)_6\cdot 7H_2O\cdot 2DMA]_n$ (**3**) $[Cu(TPPA)(NO_3)_2(H_2O)]\cdot 2H_2O]_n$ (**4**). As excepted, the self-assembly of TPPA and ancillary ligands is an effective method to generate unique architectures and topologies. Compounds **1** and **2** are both built up by TPPA and H_2bdc ligand, but they have quite different structures. Compound **1** is a 3D structure of 2-fold interpenetration, while compound **2** is a simple 2D structure. Compound **3** has a 3D non-interpenetration structure with over 24% solvent accessible void space. Compound **4** has a 2D network with different coordination mode, and the 2D networks alternate with others to form a 3D framework.

Experimental section

Materials and general methods

All compounds were charactered by X-ray powder diffraction, elemental analysis, and X-ray crystallography. All the raw materials are commercially purchased except the ligand TPPA. The thermogravimetric analyses (TGA) were performed by a Pyris 1 DSC at a heating rate of 20 °C min^{-1}. Powder X-ray diffraction (PXRD) was performed on a Bruker D8 Advance using Cu Kα radiation (1.54056 Å) at room temperature. Luminescent spectra were recorded on a Perkin Elmer LS55 fluorescence spectrophotometer at room temperature. UV-vis spectra were recorded on a Shimadzu UV–vis spectrophotometer UV-3600 at room temperature.

Synthetic procedure

Compounds **1-4** can be synthesized by a general step: a mixture of metal nitrate (0.1 mmol), TPPA (47.6 mg, 0.1 mmol) and dicarboxylic acid (0.1 mmol) was dissolved in 15 mL of a mixed solvent. The final mixture was placed in a Parr Teflon-lined stainless steel vessel (25 mL) under autogenous pressure and heated at a certain temperature for 72 hours. The detailed information of synthesis and the main features are displayed in Table 1.

Table 1 Detailed synthesis information and main features of compounds **1-4**.

Compound	Starting Chem	Temp.(°C)	Solvent (V/V)	Yield(%)	EA % (culced)	Color
1	$Co(NO_3)_2·6H_2O$+ TPPA+1,3-bdc	95	DMF-H_2O (2/3)	56	C 69.36 (69.48) H 4.10 (4.12) N 7.77 (7.91)	Dark Red
2	$Zn(NO_3)_2·6H_2O$+ TPPA+1,3-bdc	85	DMF-H_2O (2/3)	25	C 69.79 (69.74) H 4.00 (4.00) N 7.97 (7.94)	Pale Yellow

3	$Zn(NO_3)_2 \cdot 6H_2O$+ TPPA+betc	85	DMA-H_2O (2/3)	28	C 50.99 (49.89) H 4.42 (3.82) N 6.00 (5.11)	Dark Yellow
4	$Cu(NO_3)_2$+TPPA	85	DMF-H_2O(1/1)	66	C 55.22 (55.18) H 4.24 (4.21) N 11.61 (11.70)	Blue

X-ray crystallography

X-ray crystallographic data of **1**, **2** and **4** were collected at room temperature using epoxy-coated crystals mounted on glass fibers. X-ray crystallographic data of **3** was collected at room temperature by way of sealing the better single crystals in a quartz tube with mother liquor. X-ray crystallographic data of these compounds were collected on a Bruker Apex Smart CCD diffractometer with graphite-monochromated Mo-Kα radiation (λ = 0.71073 Å). Structure solutions were solved by direct methods and the non-hydrogen atoms were located from the trial structures and then refined with SHELXTL using full-matrix least-squares procedures based on F^2 values. The hydrogen atom were fixed geometrically at calculated distances and allowed to ride on the parent atoms. The relevant crystallographic data are displayed in Table 2, while the bond lengths and angles are shown in the ESI. A semiempirical absorption correction was applied using SADABS.[19] The topological analysis and some diagrams were produced using the TOPOS program.[20] CCDC numbers are 1000812-1000815 for **1** – **4**, respectively.

Results and discussion

The structure of 1

The crystal structure determination reveals that complex **1** crystallizes in the monoclinic crystal system of the *Pcca* space group. There is one Co^{2+} atom, one TPPA ligand, one deprotonated 1,3-benzenedicarboxylic acid and 1/2 H_2O molecule. The local geometry of Co^{2+} atom is depicted in Fig. 1a. The coordination environment of

the two Co^{2+} is different. One Co^{2+} atom coordinates to three N atoms from three TPPA ligands and four oxygen atoms from two 1,3-bdc^{2-} ligands, while the other Co^{2+} atom coordinates to three TPPA ligands, two oxygen atoms from two 1,3-bdc^{2-} ligands and one water molecular. Each Co^{2+} atom is connected to three TPPA ligands, while each TPPA ligand is connected to three Co^{2+} atoms, building up a 2D plane (Fig.1b). The 2D palnes are further connected by 1,3-bdc^{2-} ligands, forming a 3D network. (Fig.1c) The Co-N lengths range from 2.151(2) and 2.238(4) Å, which are similar to the values of regular values in other Co(II) complexes. The Co-O lengths range from 1.976(4) and 2.044(2) Å, also similar to the values in other ones.[20] In a single framework, there is a channel with dimensional 11.0006(46) × 17.2188(44) $Å^2$. The channel is large enough to contain another set of equivalent one, giving a 2-fold interpenetrating framework (Fig.1d). Upon interpenetrating, there is no void space calculated by PLATON.

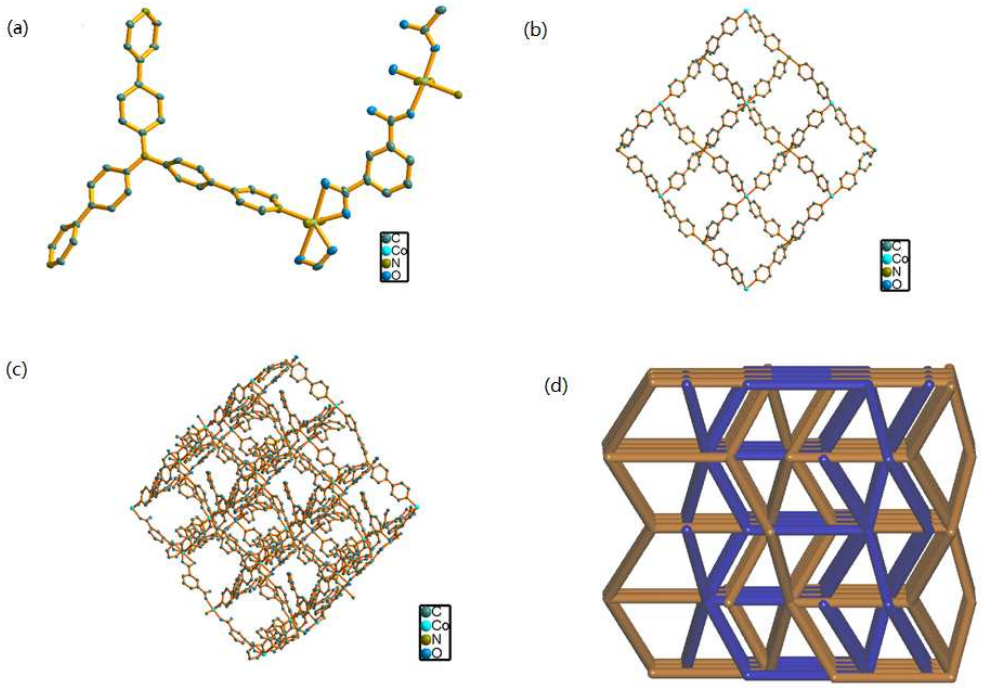

Fig. 1 (a) View of coordination environment of **1** with thermal ellipsoids shown at 30% probability. (b) View of 2D sheet built up by Co^{2+} and TPPA ligand. (c) View of 3D framework in **1**. (d) View of 2-fold interpenetrating 3D architecture in **1**.

The structure of 2

The crystal structure determination reveals that complex **2** crystallizes in the monoclinic crystal system of the *C*2/*c* space group. There is one Zn^{2+} atom, one TPPA ligand and one deprotonated 1,3-bdc^{2-} in the asymmetric unit. The local geometry of Zn^{2+} is depicted as Fig. 2a. One Zn^{2+} atom coordinates to two N atoms from two TPPA ligands and two O atoms from two 1,3-bdc ligands. Each Zn^{2+} atom connects to two TPPA ligands and each TPPA ligand connects to two Zn^{2+} atoms, building up a 1D chain, depicted as Fig.2b. The 1D chains are further connected by 1,3-bdc ligands, to form a 2D sheet (Fig.2c). The lengths of Zn-N bounds range from 2.020(4) and 2.041(4), similar to the regular values in other compounds. The lengths of Zn-O bounds range from 1.965(3) to 1.972(3), also similar to the regular values in other compounds. 2D layers accumulated to the same direction, and not be described any further. The point symbol for net is $\{4^4.6^2\}$ and the topological type is *sql*.

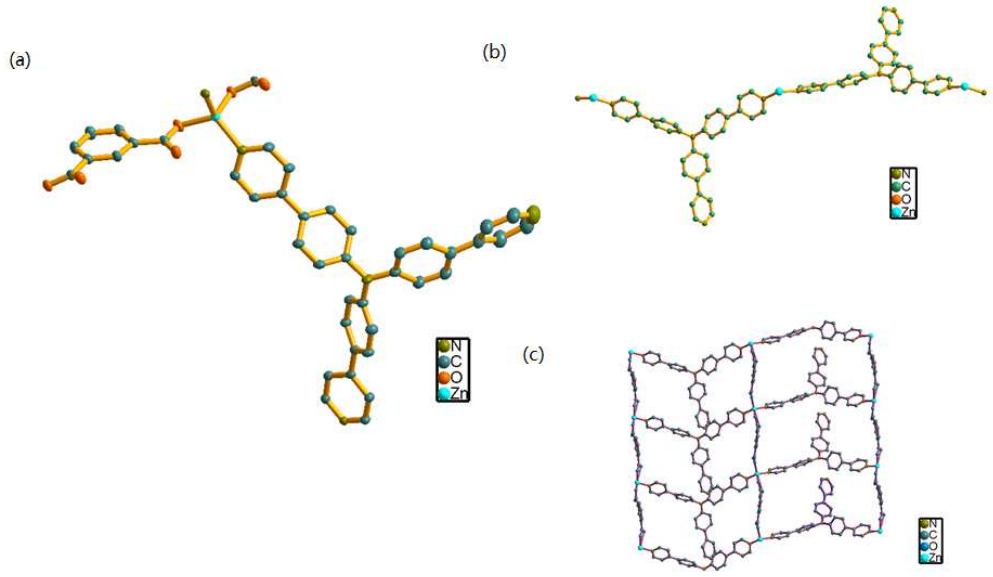

Fig. 2 (a) View of coordination environment of **2** with thermal ellipsoids shown at 30% probability. (b) View of 1D chain composed of Zn^{2+} and TPPA. (c) View of 2D sheet in **2**.

The structure of 3

The crystal structure determination reveals that complex **3** crystallizes in the triclinic crystal system of the *P-1* space group. There are three Zn^{2+} atoms, two TPPA ligands, one $Hbtec^{3-}$, 1/2 H_2btec^{2-}, 1/2 $btec^{4-}$ and three coordinated water molecules and 7/2 lattice water molecules, as well as one DMA molecule in an asymmetric unit. The local coordination environment of Zn^{2+} is depicted in Figs. 3a and 3b. The three Zn^{2+} atoms appeals different coordination environments. Zn1 connects to four atoms, including one N atom of one TPPA ligand, two O atoms from one H_2betc^{2-} and one $Hbetc^{3-}$ligands and one O atom from one water molecule. Different from Zn1, Zn2 connects to one N atom of one TPPA ligand and three O atoms from two $betc^{4-}$ ligands and one H_2betc^{2-}. Zn3 connects to four O atoms from two $betc^{4-}$ ligands two water molecules. One TPPA ligand connects to two Zn^{2+} atoms. The betc ligands appeal different coordination modes because of partly deprotonated. While all betc ligands link Zn^{2+} cations to form form a 3D structure (Fig. 3c). Finally, the betc and TPPA ligands connect the Zn atoms to form a non-interpenetrating structure (Fig.3d). The Schläfli symbol for this binodal net is $\{4.6.8^3.10\}_2\{4.6^2.8^3\}_2\{6^2.8^2.10^2\}\{6^2.8\}_2$. There is a large solvent accessible void space as large as 24.2%.

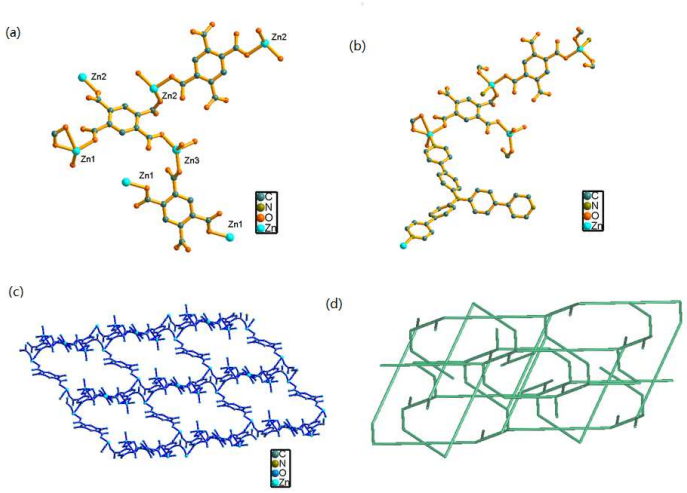

Fig. 3(a) View of asymmetric unit of **3**. (b) View of the coordination environment of Zn^{2+} and $betc^{4-}$ ligand (excluding TPPA). (c) View of the 3D framework composed of Zn^{2+} and $betc^{4-}$ ligand. (d) View of the non-interpenetrating structure of **3**.

The structure of 4

The crystal structure determination reveals that complex **4** crystallizes in the monoclinic crystal system of the $P2_1/n$ space group. There is one Cu^{2+} ion, one TPPA ligand, two nitrate ions, and two H_2O molecules in one asymmetric unit. The local coordination environment of Cu^{2+} is depicted in Fig. 4a. One Cu^{2+} connects to six atoms, including three N atoms from three TPPA ligands, two O atoms from two nitrate ligands, and one O atom from one water molecule. One TPPA ligand connects to three Cu^{2+} atoms, and one Cu^{2+} connects to three N atoms, building up a 2D sheet (Fig 4b). There are some holes in the 2D sheet, large enough to accommodate water molecules (Fig 4c). The lengths of Cu-N bounds range from 2.107(2) to 2.1324(19), which is similar to the regular value of other compounds. The lengths of Cu-O bounds range from 2.0279(19) to 2.0804(16), also similar to the values of other compounds. As shown in Fig. 4d, the Schläfli symbol for this binodal net is $\{6^3\}$ and the topology type of this net is *hcb*. And the voids are enough large so that they can be filled by other nets. Each one is catenated by two parallel adjacent identical motifs. Therefore, the whole structure is a 2D + 2D → 3D polycatenated entanglement. Up to now, there are only a few examples that increase from 2D sheets to overall 3D entanglement observed for polycatenation systems.[22]

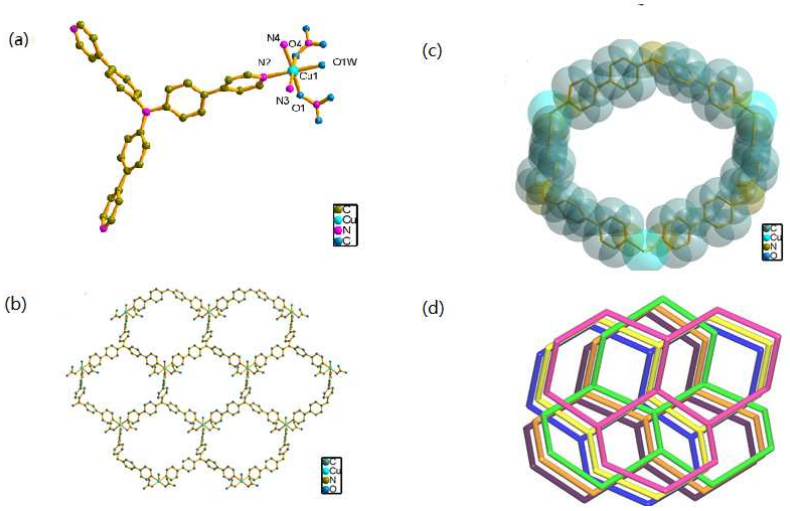

Fig.4 (a) Coordination environment of **4**. (b) View of the "hole" composed of Cu^{2+} and TPPA ligand. (c) View of the 2D sheet in **4**. (d) View of the simplified topology, packing insert of the two layers oriented towards different directions.

TGA analysis and powder X-ray diffraction

The stabilities of **1 - 4** were examined by thermogravimetric analyses (TGA) in air atmosphere from the temperature of 20 - 700 °C at the heating rate of 20 °C/min. The results indicate that all the three MOFs are stable in air atmosphere (Fig. 5). Compound **1** did not obviously lose weight below 490 °C, then collapse at 490 °C, indicating there is no guest molecule in the structure of compound **1**. For compound **2**, there is a weight loss of 1.811% under 100 °C. There is neither void space nor guest molecules in the structure of **2**. In our opinion, some water or other guest molecules are absorbed in the surface of the powder, which is easy to lose below 100 °C. Compound **2** is also thermo-stable, for there is no further weight loss until 420 °C. For compound **3**, a weight loss of 11.307% occurs below 150 °C. The results indicates that there are 7/2 molecules and 1 DMA molecule in an asymmetric unit. (calced 10.949%). Compound **3** is less stable than the other three, collapsing at 300 °C. Compound **4** acted quite different, it lost 4.909% (calced 5.016%) weight during 120 and 170 °C, indicating a loss of two non-coordinated water molecules. Then a 2.347% (calced 2.508%) weight loss occurs between 210 and 230 °C, indicating a loss of one coordinated water molecule. A further weight loss of 8.760% (calced 8.634%) occurs between 280 and 300 °C, indicating a loss of NO_3^-. The structure collapse at 390 °C.

For compound **1, 2 and 4**, the X-ray diffraction is very similar to the simulated data. For compound **3**, the experimental data acts quite different from the simulated one. Thus occurs when the single crystal is easy to effloresce in atmosphere. The simulated data is simulated by the original single crystal, but some of the observed data is observed after efflorescence. (Fig. S1)

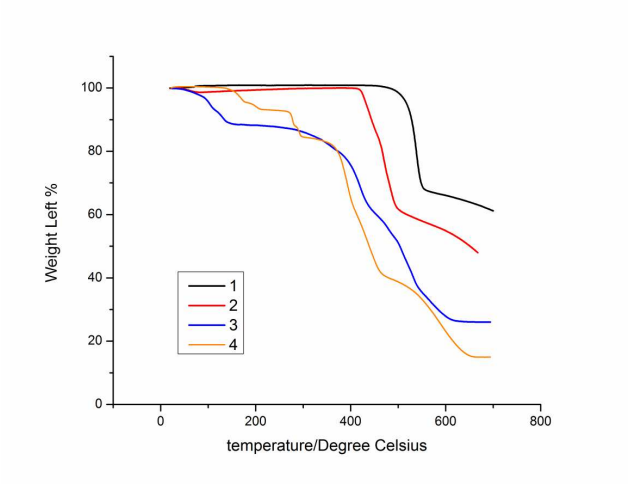

Fig. 5 TGA analysis of compounds **1 - 4**.

Optical properties

Only the UV-vis absorption spectra of **1** and **4** were carried out at room temperature (Figs. 6 and 7). The Co-centered MOF **1** exhibits a strong absorption at 340 nm, which can be considered as ligand–metal charge-transfer (LMCT) transitions. Both the MOF **1** and the free TPPA ligand exhibits an absorption at 230~260 nm, which can be assigned as $\pi \rightarrow \pi^*$ transitions. There is a weak absorption at 580 nm, which can be considered as d-d transition. For the Cu-centered MOF **4**, $\pi \rightarrow \pi^*$ transitions also locate at 230~260 nm. A weak absorption locates at 625 nm, which can be considered as d-d transition. Different from Co-centered, the LMCT transition at 340 nm is much weaker.

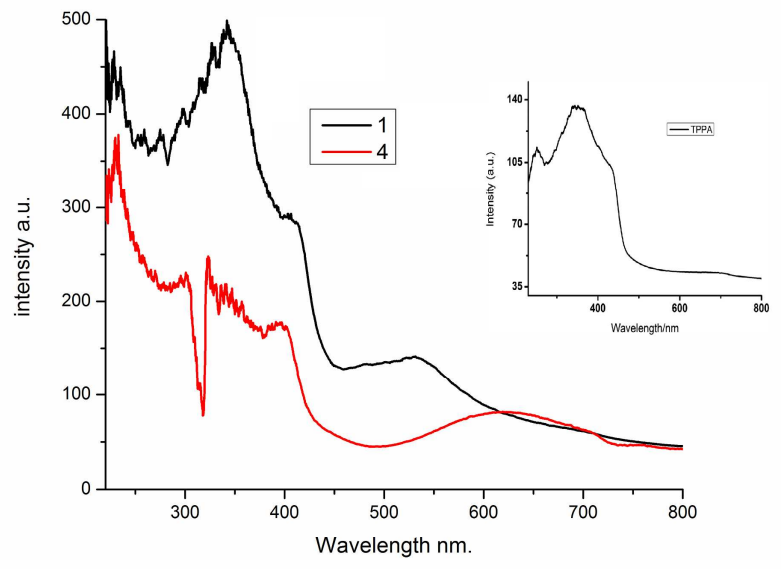

Fig. 6 Solid-state UV-vis spectra of the Co-centered compounds **1** and **4** and TPPA ligand at room temperature.

Luminescent compounds are of great interest because there may be various applications in chemical sensors[21], photochemistry, etc[22]. Only the luminescent spectrum of **2** is taken (for compound **3** is not stable). Compared to the fluorescence spectroscopy of free TPPA (λ_{em}= 525 nm at the excitation wavelength of 420nm), the solid-state fluorescence spectrum of compound **2** only has a minor shift. As shown in the Fig.7, the luminescent emmission of compound **2** is caused by the TPPA ligand.

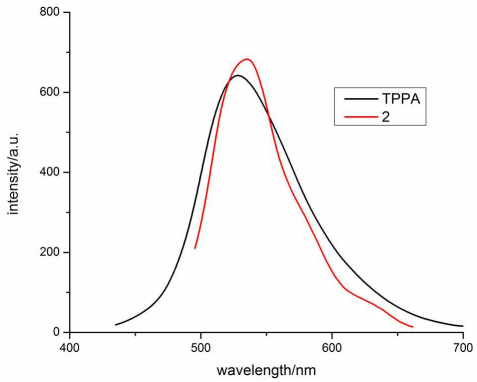

Fig. 7 Emission spectra of Zn-centered compound **2** and free TPPA at room temperature.

Conclusions

In conclusion, four novel MOFs based on triangle ligand TPPA have been synthesized, three of which are stable in atmosphere. Compound **1** has a 2-fold interpenetrating 3D structure with symbol for net $\{6^3\}\{6^8.8^2\}$. Compound **2** is a 2D framework. The coordination mode of TPPA in **2** is different from which of **1**, only two N atoms of three pyridine rings are connected to the metal ions. For compounds **1** and **2**, there is only a difference in the metal ions, but the resulting structures are quite different. Compound **3** has a non-interpenetrated 3D structure, with void space up to 24.2%, symboling $\{4.6.8^3.10\}_2\{4.6^2.8^3\}_2\{6^2.8^2.10^2\}\{6^2.8\}_2$. Compound **4** does not contain carboxylate ligands, but nitrate ligand. Different from compounds **1-3**, compound **4** shows a 2D → 3D framework with parallel polycatenation. The results indicate that the change of metal ions and the introduction of ancillary ligands show significant effects on the resulting structures.

Associates content

Supporting information available.

Selected bond lengths and angles, complementary drawings for crystal structures, simulated, experimental X-ray powder diffraction patterns, and CCDC references: CCDC 1000812-1000815. These materials are available free of charge via the Internet at http://pubs.rsc.org.

Acknowledgements

This work was supported by grants from the Natural Science Foundation of China 21371092; 91022011), and National Basic Research Program of China (2010CB923303).

Notes and references

(1) (a)Y. Cui, Y. Yue, G. Qian, B. Chen, *Chem. Rev.* 2012, **112**, 1126. (b) L. J. Murray, M. Dincâ, J. R. Long, *Chem. Soc. Rev.* 2009, **38**, 1294. (*c*) Q. X. Jia, H. Tian, J. Y. Zhang, E. Q. Gao, *Chem. Eur. J.* 2011, **17**, 1040. (d) R. Spencer, Ahrenholtz,

C. Charity, Epley, J. Morris, Amanda *J. Am. Chem. Soc.* 2014, **136**, 2464. (e) G. Givaja, P. Amo-Ochoa, C. J. Gomez-Garcia, F. Zamora, *Chem. Soc. Rev***.** 2012, **41**, 115. (f) B. Y. Li, Y. M. Zhang, D. X. Ma, T. L. Ma, Z. Shi, S.Q. Ma, *J. Am. Chem. Soc*. 2014, **136**, 1202.

(2) (*a*) Y. Cui, O. R. Evans, H. L. Ngo, P. S. White, W. B. Lin, *Angew. Chem., Int. Ed.* 2002, **41**, 1159. (*b*) O. M. Yaghi, M. O'Keeffe, N. W. Ockwig, H. K. Chae, M. Eddaoudi, J. Kim, *Nature* 2003, **423**, 705. (c) L. Qin, J. S. Hu, Y. Z. Li, H. G. Zheng, *Cryst. Growth Des.* 2012, **12**, 403. (d) Y. Peng, V. Krungleviciute, I. Eryazici, J. T. Hupp, O. K. Farha, T. Yildirim, *J. Am. Chem. Soc*. 2013, **135**, 11887. (e) H. Wu, Q. Gong D. H. Olson, J. Li, *Chem. Rev*. 2012, **112**, 836.

(3) (a) S. Wang, R. R. Yun, Y. Peng, Q. Zhang, J. Lu, J. Dou, J. Bai, D. Li, D. Wang, *Cryst. Growth Des.* 2012, **12**, 79. (b) R. W. Larsen, L. Wojtas, *J. Phys. Chem. A* 2012, **116**, 7830. (c) R. W. Larsen, L. Wojtas, J. Perman, R. L. Musselman, M. J. Zaworotko, C. M. Vetromile, *J. Am. Chem. Soc*. 2011**,** **133**, 10356. (d) T. C. Narayan, T. Miyakai, S. Seki, M. Dincă, *J. Am. Chem. Soc.* 2012**,** **134**, 12932

(4) (a) K. J. Balkus. Jr, A. G. Gabrielov, S. L Bell, F. Bedioui, L. Roué, J. Devynck, *Inorg. Chem*. 1994, **33**, 67. (b) M. Yoshizawa, T. Kusukawa, M. Fujita, K. Yamaguchi, *J. Am. Chem. Soc*. 2000, **122**, 6311.

(5) (a) T. Bogaerts, A. Van Yperen-De Deyne, Y. Y. Liu, F. Lynen, V. Van Speybroeck, P. Van Der Voort, *Chem. Commun*. 2013, **49**, 8021. (b) J. Yu, Y. Cui, C. Wu, Y. Yang, Z. Wang, M. O'Keeffe, B. Chen, G. Qian, *Angew. Chem., Int. Ed*. 2012, **51**, 10542. (c) J. Juan-Alcañiz, J. Gascon, F. Kapteijn, *J. Mater. Chem*. 2012, **22**, 10102. (d) H. Peng, W. Chen, Y. Cheng, L. Hakuna, R. Strongin, B. Wang, *Sensors* 2012, **12**, 15907 (e) N. Kumar, V. Bhalla, M. C. Kumar, *Chem. Rev*. 2013, **257**, 2335.

(6) (*a*) B. Moulton, M. J. Zaworotko, *Chem. Rev.* 2001, **101**, 1629. (*b*) S. A. Barnett, A. J. Blake, N. R. Champness, C. Wilson, *Chem. Commun.* 2002, 1640. (c) L. A. Montoya, T. F. Pearce, R. J. Hansen, L. N. Zakharov, M. D. Pluth, *J. Org. Chem*. 2013, **78**, 6550. (d) W. Ki, J. Li, *J. Am. Chem. Soc*. 2008, **130**, 8114.

(7) K. K. W. Lo, B. T. N, Chan, H. W. Liu, K. Y. Zhang, S. P. Y. Li, T. S. M. Tang,

Chem Commun. 2013, **49**, 4271.

(8) (*a*) T. L. Hennigar, D. C. MacQuarrie, P. Losier, R. D. Rogers, M. J. Zaworotko, *Angew. Chem., Int. Ed. Engl.* 1997, **36**, 972. (*b*) H. Abourahma, B. Moulton, V. Kravtsov, M. J. Zaworotko, *J. Am. Chem. Soc.* 2002, **124**, 9990; (*c*) L. Jiang, T. B. Lu, X. L. Feng, *Inorg. Chem.* 2005, **44**, 7056. (d) A. M. Chippindale, S. M. Cheyne, S. J. Hibble, *Angew. Chem., Int. Ed.* 2005, **44**, 7942.

(9) (a) M. S. Wang, G. C. Guo, W. T. Chen, G. Xu, W. W. Zhou, K. J. Wu, J. S. Huang, *Angew. Chem., Int. Ed*. 2007, **46**, 3909.(b) W. Ki, J. Li, *J. Am. Chem. Soc.* 2008, **130**, 8114. (c) K. T. Kamtekar, A. P. Monkman, M. R. Bryce, *Adv. Mater*. 2010, **22**, 572. (d) J. Karpiuk, E. Karolak, J. Nowacki, *Phys. Chem. Chem. Phys*. 2010, **12**, 8804. (e) R. Varghese, H. A. Wagenknecht, *Chem. Eur. J*. 2009, **15**, 9307. (f) J. He, M. Zeller, A. D. Hunter, Z. Xu, *J. Am. Chem. Soc*. 2012, **134**, 1553.

(10) (*a*) H. Wu, H. Y. Liu, Y. Y. Liu, J. Yang, B. Liu, J. F. Ma, *Chem. Commun.* 2011, 1818. (*b*) H. Wu, H. Y. Liu, B. Liu, J. Yang, Y. Y. Liu, J. F. Ma, Y. Y. Liu, H. Y. Bai, *Cryst. Eng. Comm.* 2011, **13**, 3402. (c) P. Pandey, O. K. Farha, A. M. Spokoyny, C. A. Mirkin, M. G. Kanatzidis, J. T. Hupp, S. B. T. Nguyen, *J. Mater. Chem*. 2011, **21**, 1700. (d) P. M. Budd, E. S. Elabas, B. S. Ghanem, S. Makhseed, N. B. McKeown, K. J. Msayib, C. E. Tattershall, D. Wang, *Adv. Mater*. 2004, **16**, 456.

(11) M. D. Zhang, C. M. Di, L. Qin, X. Q. Yao, Y. Z. Li, Z. J. Guo, H. G. Zheng, *Cryst. Growth Des.* 2012, **12**, 3957.

(12) (a) E. C. Spencer, R. J. Angel, N. L. Ross, B. E. Hanson, J. A. K. Howard, *J. Am. Chem. Soc*. 2009, **131**, 4022. (b) B. Li, Y. Zhang, D. Ma, L. Li, G. Li, G. Li, Z. Shi, S. Feng, *Chem. Commun*. 2012, **48**, 6151. (c) P. Li, S. Regati, R. J. Butcher, H. D. Arman, Z. Chen, S. Xiang, B. Chen, C. G. Zhao, *Tetrahedron Lett*. 2011, **52**, 6220.

(13) (a) M. H. Alkordi, Y. Liu, R. W. Larsen, J. F. Eubank, M. Eddaoudi, *J. Am. Chem. Soc.* 2008, **130**, 12639 (b) S. S. Y. Chui, S. M. F. Lo, J. P. H. Charmant, A. G. Orpen, I. D. Williams, *Science* 1999, **283**, 1148. (c) M. Ma, D. Zacher, X. N. Zhang, R. A. Fischer, N. Metzler-Nolte, *Cryst. Growth Des*. 2011, **11**, 185. (d) N.

Reimer, B. Gil, B. Marszalek, N. Stock, *CrystEngComm* 2012, **14**, 4119. (e) Y. Zhou, B. Yan, *CrystEngComm* 2013, **15**, 5694. (f) M. Roushan, X. Zhang, J. Li, *Angew. Chem., Int. Ed.* 2012, **51**, 436. (g) J. M. Chin, E. Y. Chen, A. G. Menon, H. Y. Tan, A. T. S. Hor, M. K. Schreyer, J. W. Xu, *CrystEngComm* 2013, **15**, 654. (h) D. F. Sava, L. E. S. Rohwer, M. A. Rodriguez, T. M. Nenoff, *J. Am. Chem. Soc*. 2012, **134**, 3983.

(14) (a) C. Y. Sun, X. L. Wang, X. Zhang, C. Qin, P. Li, Z. M. Su, D. X. Zhu, G. G. Shan, K. Z. Shao, H. Wu, J. Li, *Nat. Commun*. 2013, **4**, 2717. (b) H. L. Guo, Y. Z. Zhu, S. Wang, S. Q. Su, L. Zhou, H. Zhang, *J. Chem. Mater*. 2012, **24**, 444. (c) T. Lescouet, E. Kockrick, G. Bergeret, M. Pera-Titus, S. Aguado, D. Farrusseng, *J. Mater. Chem*. 2012, **22**, 10287 (d) L. S. Grajciar, O. Buldsky, P. Nachtigall, *J. Phys. Chem. Lett*. 2010, **1**, 3354.

(15) (a) K. M. Gupta, Z. Q. Hu, J. W. Jiang, *RSC Adv*. 2013, **3**, 12794. (b) Y. Le Moullec, M. Kanniche, *Int. J. Greenhouse Gas Control* 2011, **5**, 727.

(16) D. F. Sun, S. Q. Ma, Y. X. Ke, D. J. Collins, H. C. Zhou, *J. Am. Chem. Soc*. 2006, **128**, 3896.

(17) S. Sakashita, M. Takizawa, J. Sugai, H. Ito, Y. Yamamoto, *Org. Lett.* 2013, **15**, 4308.

(18) (a) J. C. Dai, X. T. Wu, Z. Y. Fu, C. P. Cui, S. M. Hu, W. X. Du, L. M. Wu, H. H. Zhang, R. Q. Sun, *Inorg. Chem*. 2002, **41**, 1391. (b) F. D. Meng, L. Qin, M. D. Zhang, H. G. Zheng, *CryEngComm.* 2014, **16**, 698.

(19) Bruker 2000, SMART (Version 5.0), SAINT-plus (Version 6), SHELXTL(Version 6.1), and SADABS (Version 2.03); Bruker AXS Inc.: Madison, WI.

(20) V. A. Blatov, A. P. Shevchenko, V. N. Serezhkin, *J. Appl. Crystallogr.* 2000, **33**, 1193.

(21) (a) L. L. Liang, S. B. Ren, J. Zhang, Y. Z. Li, H. B. Du and X. Z. You, *Cryst. Growth Des.*, 2010, **10**, 1307 (b) T. L. Greaves, C. J. Drummond, *Chem. Soc. Rev*. 2013, **42**, 1096. (c) Y. Y. Gu, S. P. Zhang, L. Martinetti, K. H. Lee, L. D. Mclntosh, C. D. Frisbie, T. P. Lodge, *J. Am. Chem. Soc*. 2013, **135**, 9652. (d) A. I.

Cooper, *Angew. Chem., Int. Ed*. 2012, **51**, 7892.

(22) (a) R. V. Jagadeesh, H. Junge, M. M. Pohl, J. Radnik, A. Brückner, M. Beller, *J. Am. Chem. Soc*. 2013, **135**, 10776. (b) R. K. Totten, Y. S. Kim, M. H. Weston, O. K. Farha, J. T. Hupp, S. T. Nguyen, *J. Am. Chem. Soc*. 2013, **135**, 11720. (c) S. Kopilevich, A. Gil, M. Garcia-Ratés, J. Bonet-Ávalos, C. Bo, A. Müller, I. A. Weinstock, *J. Am. Chem. Soc.* 2012, **134**, 13082.

(23) (a) J. P. Zhang, Y. Y. Lin, W. X. Zhang, X. M. Chen, *J. Am. Chem.Soc.* 2005, **127**, 14162 (b) S. B. Choi, H. Furukawa, H. J. Nam, D. Y. Jung, Y. H. Jhon, A. Walton, D. Book, M. O'Keeffe, O. M. Yaghi, J. Kim, *Angew.Chem., Int. Ed*. 2012, **51**, 8791.

Table 2. Crystal data and structural refinements parameters of complexes **1-4**

Frameworks	**1**	**2**	**3**	**4**
formula	$Co_2C_{82}H_{58}N_8O_9$	$ZnC_{41}H_{28}N_4O_4$	$Zn_6C_{114}H_{90}N_{10}O_{47}$	$CuC_{33}H_{30}N_6O_9$
formula weight	1417.22	706.04	2744.18	718.17
crystal system	orthorhombic	monoclinic	triclinic	monoclinic
space group	*pcca*	*C2/c*	$P\,\bar{1}$	$P2_1/n$
a (Å)	13.6179(9)	20.332(2)	15.1690(9)	17.676(4)
b (Å)	14.7639(10)	10.0941(11)	15.4530(9)	8.814(3)
c (Å)	33.973(2)	32.682(4)	16.4504(8)	24.121(4)
α (deg)	90.00	90.00	67.469(2)	90.00
β (deg)	90.00	96.688(2)	80.559(2)	93.010(4)
γ (deg)	90.00	90.00	61.982(7)	90.00
Z	4	8	1	4
V (Å^3)	6830.4(8)	6661.9(13)	3143.7(3)	3752.8(17)
D_{calcd}(g cm^{-3})	1.378	1.408	1.450	1.271
μ(Mo Ka)(mm-1)	0.553	0.787	1.217	0.638
F(000)	2928	2912	1391	1484
temperature (K)	291(2)	296(2)	291(2)	292(2)
theta min-max (deg)	1.38, 25.99	2.25, 24.71	1.34, 25.00	1.39, 27.69
tot., uniq. data	52829, 6711	23139, 5655	23838,11058	33332, 8683
R(int)	0.0206	0.0709	0.0639	0.0866
observed data [$I > 2\sigma(I)$]	4549	4237	9305	5809
Nref, Npar	6711, 462	5655, 451	11058, 832	8683, 457
R1,*wR2* (all data)	0.0614, 0.1896	0.0664, 0.1966	0.0593, 0.1573	0.0485, 0.1166
S	1.096	1.038	1.017	0.956
min. and max rest dens (e	-0.632, 0.598	-0.780, 0.997	-0.587, 0.575	-0.380, 0.843

$R_1 = \Sigma||F_o|-|F_c||/\Sigma|F_o|$. $wR_2 = \{\Sigma[w(F_o^2-F_c^2)^2]/\Sigma[w(F_o^2)^2]\}^{1/2}$; where $w = 1/[\sigma^2(F_o^2)+(aP)^2+bP]$, $P = (F_o^2+2F_c^2)/3$

A series of MOFs based on a triangle ligand tri(4-pyridylphenyl)amine combined with carboxylate or nitrate auxiliary ligand

Fandian Meng, Mingdao Zhang, Kang Shen, Yizhi Li and Hegen Zheng*

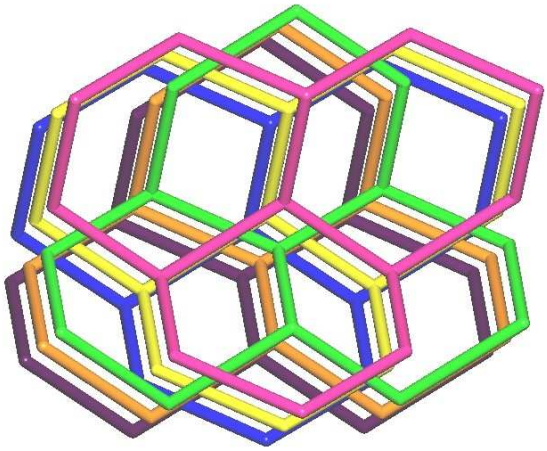

A series of new metal-organic frameworks that have novel structures and features based on a triangle ligand tri(4-pyridylphenyl)amine (TPPA) have been successfully synthesized and structurally characterized in detail.